HHS Public Access

Author manuscript

J Mol Biol. Author manuscript; available in PMC 2017 March 14.

Published in final edited form as:

J Mol Biol. 2017 January 20; 429(2): 237–248. doi:10.1016/j.jmb.2016.11.030.

Structural basis of Arp2/3 complex inhibition by GMF, Coronin, and Arpin

Olga S. Sokolova[1], **Angelina Chemeris**[1,5], **Siyang Guo**[2], **Salvatore L. Alioto**[2], **Meghal Gandhi**[2], **Shae Padrick**[3], **Evgeniya Pechnikova**[4], **Violaine David**[5], **Alexis Gautreau**[5], and **Bruce L. Goode**[2,*]

[1]Department of Biology, Moscow M.V. Lomonosov University, 119234, Moscow, Russia

[2]Department of Biology, Brandeis University, Waltham, MA 02453 USA

[3]Department of Biochemistry and Molecular Biology, Drexel University College of Medicine, Philadelphia, PA 19102 USA

[4]V.A. Shoubnikov Institute of Crystallography RAS, 119333, Moscow, Russia

[5]Ecole Polytechnique, CNRS UMR7654, 91120, Palaiseau, France

Abstract

The evolutionarily conserved Arp2/3 complex plays a central role in nucleating the branched actin filament arrays that drive cell migration, endocytosis, and other processes. To better understand Arp2/3 complex regulation, we used single particle electron microscopy to compare the structures of Arp2/3 complex bound to three different inhibitory ligands: GMF, Coronin, and Arpin. Although the three inhibitors have distinct binding sites on Arp2/3 complex, they each induced an 'open' nucleation-inactive conformation. Coronin promoted a standard (previously described) open conformation of Arp2/3 complex, with the N-terminal β-propeller domain of Coronin positioned near the p35/ARPC2 subunit of Arp2/3 complex. GMF induced two distinct open conformations of Arp2/3 complex, which correlated with two suggested binding sites for GMF. Further, GMF synergized with Coronin in inhibiting actin nucleation by Arp2/3 complex. Arpin, which uses VCA-related acidic (A) motifs to interact with the Arp2/3 complex, induced the standard open conformation, and two new masses appeared at positions near Arp2 and Arp3. Further, Arpin showed additive inhibitory effects on Arp2/3 complex with Coronin and GMF. Together, these data suggest that Arp2/3 complex conformation is highly polymorphic and that its activities can be controlled combinatorially by different inhibitory ligands.

Keywords

actin nucleation; single particle EM; yeast; conformation

*Corresponding author: goode@brandeis.edu.

INTRODUCTION

Dynamic reorganization of the actin cytoskeleton is vital to cell and tissue morphogenesis, and to processes such as cell motility, endocyosis, inflammatory responses, wound healing, neuronal activity, and intracellular transport [1–3]. Central to these rearrangements of the actin cytoskeleton is the *de novo* formation of new filaments by actin nucleation mechanisms. One of the most important and conserved nucleators of new actin filaments is the actin-related protein (Arp)2/3 complex, which specifically assembles branched filament arrays [4–6]. Due to the potency of its nucleation capabilities, the Arp2/3 complex must be tightly controlled in vivo. This is achieved by several known strategies. First, strong nucleation by Arp2/3 complex requires its association with a stimulatory co-factor or nucleation-promoting factor (NPF), the best characterized of which are the WASP/WAVE family proteins [7]. Second, nucleation by Arp2/3 complex can be inhibited by some binding partners, including Coronin [8–11], Glia Maturation factor (GMF) [12–14], Gadkin [15], and Arpin [16]. While significant advances have been made in defining the structural basis of Arp2/3 activation both in solution and on actin filaments [17–20], there remains limited understanding of how Arp2/3 complex is inhibited.

Unbound (ligand-free) yeast and bovine Arp2/3 complexes exist in equilibrium between two distinct conformational states, open (inactive) and closed (primed for nucleation) [20–22]. Interactions with NPFs can shift the conformational distribution of Arp2/3 complex molecules toward the closed state [20, 21]. These interactions also enhance Arp2/3 complex binding to the side of an existing (mother) filament, leading to nucleation of a new (daughter) filament at a 70° angle [19, 23–27]. Importantly, even in the absence of NPFs, Arp2/3 complex has some inherent nucleation activity, and possibly for this reason cells additionally express inhibitory ligands of Arp2/3 complex such as Coronin, GMF, and Arpin.

The Arp2/3 complex has a conserved architecture, consisting of two actin-related proteins (Arp2 and Arp3) and five additional subunits [4]: ARPC1 (p40), ARPC2 (p35), ARPC3 (p21), ARPC4 (p19), ARPC5 (p15). Different subunits in the complex contribute in different ways to Arp2/3 complex function and regulation, including NPF binding [20] and/or participation in joining mother and daughter filaments [19]. Many NPFs, including WASP, Scar/WAVE, WASH proteins, possess a short segment at their C-terminus called the ‘VCA’ domain, which consists of a WH2 or ‘V’ (WASp-homology 2 or Verprolin homology) domain, a ‘C’ motif (Central), and an ‘A’ motif (Acidic). The V portion of VCA binds G-actin, while the CA portion binds Arp2/3 complex. Free VCA is unstructured, but may acquire secondary structure upon contacting Arp2/3 complex [28]. Each Arp2/3 complex can bind two VCA domains via separate surfaces [28–30]. Electron tomography at actin filament branch junctions suggests that Arp2/3 complex undergoes additional conformational changes during daughter filament nucleation. In the final branch site, Arp2/3 complex forms a stable link between the side of the mother filament and the pointed end of the daughter filament [19].

Among the three above-mentioned inhibitors of Arp2/3 complex, the first identified was Coronin [8]. Subsequently, *S. cerevisiae* Coronin (Crn1) was shown to bind near the p35/

ARPC2 subunit and dramatically shift the distribution of Arp2/3 complex toward the open/inactive state [21]. Mammalian homologs of Coronin similarly inhibit Arp2/3 complex [9, 10], presumably through a similar mechanism. The second Arp2/3 inhibitor identified was GMF (18 kDa), which is conserved from yeast to humans and has a fold similar to ADF/cofilin proteins [31]. However, rather than binding to actin like ADF/cofilin, GMF binds directly to Arp2/3 complex via interactions with the Arp2 and p40/ARPC1 subunits [12–14]. Through these interactions, GMF inhibits actin nucleation by Arp2/3 complex, and catalyzes the dissociation of daughter filaments from mother filaments, i.e., debranching [13, 32, 33]. A co-crystal structure of GMF-bound Arp2/3 complex revealed that one of the GMF binding sites to be located on the Arp2 and ARPC1/p40 subunits [14]. However, binding saturation analysis, chemical crosslinking, and molecular modeling all suggested that there may be a second, weaker binding site that involves interactions with Arp3 [13]. The third Arp2/3 inhibitor identified was Arpin, which posesses an A-motif that competitively blocks the stimulatory effects of VCA to control leading edge actin network dynamics and cell migration in vivo [16]. Together, these observations have raised new questions about the structural and mechanistic basis of these inhibitors, including: (1) How does each inhibitor affect Arp2/3 complex conformation? (2) How many GMF- and Arpin-binding sites are on the Arp2/3 complex, and what is the relationship between where they bind and how they affect Arp2/3 conformation? (3) Can pairs of inhibitors synergize in blocking nucleation by Arp2/3 complex?

Here we used single particle electron microscopy to determine 2D and 3D structures of *S. cerevisiae* Arp2/3 complex bound separately to GMF and Arpin, and compare them to our previously defined Coronin-bound structure [21]. This analysis has revealed key similarities and differences in the interactions of the different inhibitors. Further, we demonstrate that Coronin and GMF synergize in suppressing actin nucleation by Arp2/3 complex, and that Arpin exhibits compounded effects on Arp2/3 complex in the presence of Coronin or GMF.

RESULTS

Effects of Gmf1, Arpin, and GST-Crn1 on Arp2/3 complex conformation

As a first step toward understanding the structural basis for Arp2/3 inhibition by GMF, Arpin, and Coronin, we used single particle EM analysis to generate 2D projection images of free and ligand-bound Arp2/3 complexes. The Arp2/3 complex is known to adhere to EM grids by a flat surface, making 2D projections a useful analysis. For this work, we used *S. cerevisiae* Arp2/3 complex, which is more amenable to conformational analysis by EM than bovine Arp2/3 [21], the yeast homologs of GMF (Gmf1) and Coronin (Crn1), and human Arpin. By using yeast Arp2/3 complex, we were able to integrate a C-terminal 3HA-TEV tag, isolate the Arp2/3 complex on HA-antibody-coated beads, load different ligands (Gmf1, GST-Crn1, and Arpin), and TEV protease release the Arp2/3-ligand complexes for EM imaging. This reduced the background of free ligand on the EM grids. Importantly, human Arpin was able to inhibit actin nucleation by yeast Arp2/3 complex (Fig. S1), similar to its effects on mammalian Arp2/3 complex [16].

Consistent with our previous studies [21], we observed that free yeast Arp2/3 complex adopted different conformations. We used hierarchal ascendant classification in IMAGIC5

software followed by summing the particles into 50 classes, as described in Methods. Approximately 60% of the particles in Arp2/3 complex alone samples had a cleft between the Arp2 and Arp3 subunits, classifying them as the ‘open’ (inactive) conformation, whereas the remaining ~40% of particles lacked a visible cleft, classifying them as the ‘closed’ (primed for nucleation) conformation (Fig. 1A and 1B). Addition of each inhibitor skewed Arp2/3 conformational distribution toward the open/inactive state (Fig. 1B). These results suggest that the three inhibitors induce related conformational changes in Arp2/3 complex.

GST-Crn1 position on Arp2/3 complex

Next, we attempted to locate GST-Crn1 on the surface of Arp2/3 complex by comparing 2D projection images for free and ligand-bound Arp2/3 complexes (Fig. 1C). Our previous work showed that binding of untagged Crn1 monomer to Arp2/3 complex produces a single new mass located near the p35/ARPC2 subunit [21], agreeing with two-hybrid interactions between the C-terminus of Crn1 and p35/ARPC2 [8]. This ~5 nm diameter single new mass presumably corresponds to the globular N-terminal beta-propeller domain (~40 kDa) of Crn1. In contrast, the C-terminus of Crn1, which contacts the p35/ARPC2 subunit, was not visible, possibly because it lacks sufficient mass and/or tertiary structure. In the current experiments, using artificially dimerized GST-Crn1, we were able to expand on our previous findings. We detected two masses of a similar size near the p35/ARPC2 subunit (Fig. 1C, arrows), in the majority of cases (14 out of 20 class averages), consistent with the presence of two Crn1 beta-propeller domains linked together by a smaller GST dimer, which possibly contributes to these masses. The distance between each of the two large masses and the surface of the Arp2/3 complex was 10–15 nm, similar to the distance we previously observed for the single mass using untagged Crn1 [21].

Free Crn1 in solution readily oligomerizes via homophilic interactions of its C-terminal coiled coil domain [34], which is a conserved feature in Coronins from other species [35, 36]. However, in our previous work we never observed more than a single Crn1 molecule bound to Arp2/3 complex [21], and here using artificially dimerized GST-Crn1 we instead observed two molecules bound to each complex in most cases. The simplest interpretation is that one Crn1 molecule in the GST-Crn1 dimer is bound to Arp2/3 complex while the other is free, as depicted in our cartoon representation (Fig. 1C, right). Together, these observations support the view of a single Crn1-binding site on Arp2/3 complex, mediated by the Crn1 coiled-coil domain, and suggest further that Crn1 may bind Arp2/3 complex as a monomer because coiled-coil-dependent oligomerization and coiled-coil-dependent Arp2/3 binding are mutually exclusive [8, 34].

Two distinct 3D structures of Gmf1-bound Arp2/3 complex

Crn1 (GST-tagged) and untagged Arpin each induced a ‘standard’ open structure, characterized by a visible and pronounced p21/ARPC3 subunit in 2D projections, as described for untagged Crn1 [21]. However, untagged Gmf1 induced two separate open conformations (Fig. 2A): (1) a ‘standard’ open conformation, and (2) a new open conformation, in which the p21/ARPC3 subunit has undergone a major shift in its position as highlighted by the difference map between these two conformations (Fig. 2A, bottom row, orange arrowheads). We solved the 3D structures of each Gmf1-induced open

conformation (Fig. 2C & 2D). Tilted pairs of images (2400 individual particles) were processed to obtain 100 class averages (representative classes in Fig. S5A), from which we solved the 3D structures. To aid in the interpretation, we derived a 3D map of the co-crystal structure of GMF-bound Arp2/3 complex [14] filtered at 25 Å resolution (Fig. 2B). This crystal structure includes an intact Arp2 subunit, whereas previous structures lacked a portion of Arp2 [14]. Importantly, this structure was never used here for refining the 3D reconstructions, and is shown only for comparative purposes.

Our 3D reconstructions of the two open conformations of Arp2/3 complex induced by GMF (Fig. 2B & 2C) confirmed the major structural changes observed in our 2D projections (Fig. 2A). In the Gmf1-bound new open conformation there was a major rearrangement of the p21/ARPC3 subunit, which pivots to a new position behind Arp3, explaining why it was not visible in our 2D projections. In the 3D reconstruction of the Gmf1-bound standard open conformation, there was a more modest shift of the p21/ARPC3 subunit in the same direction. In both Gmf1-bound open conformations, there was substantial rotation of the p35/ARPC2 subunit, perhaps accompanying the mentioned shift in the p21/ARPC3 subunit. Indeed, mutational studies of p35/ARPC2 have suggested that this subunit binds directly to mother filament sides and mediates both inhibitor- and activator-induced structural rearrangements of other subunits in the complex [14, 21, 37]. In each 3D reconstruction, we also observed at least one new mass roughly the size of Gmf1 (Fig. 2C & 2D, pink masses; also see difference maps in Fig. S3). In the standard open conformation, a clear new mass appeared in the same position as GMF in the co-crystal (grey shading in Fig. 2B). In the new open conformation (Fig. 2D), this mass on Arp2 and p40/ARPC1 was absent, but a new mass appeared in a distinct location, on Arp3. Interestingly, the standard open conformation induced by GMF showed a less prominent new mass at the second location (Fig. S3C). This observation raises the possibility that only a subset of the particles analyzed to obtain this structure had a GMF bound at the second site. All together, these data suggest that GMF induces two distinct open conformations in Arp2/3 complex, likely arising from interactions of GMF at distinct binding sites on Arp2/3 complex.

In addition, we attempted to map the Gmf1 binding site(s) on Arp2/3 complex by analyzing 2D projections of Gmf1-GFP-bound Arp2/3 complexes. This revealed variable positions for GFP tag (25 kDa) (Fig. S2A), but it was difficult to locate the Gmf1 portion of Gmf1-GFP because of its smaller mass (17 kDa) and because it directly contacts the complex. The Gmf1-GFP fusion used includes a 13 residue-long linker connecting Gmf1 and GFP, which would allow for a gap of 3–5 nm between GFP and Gmf1 on Arp2/3 complex. Consistent with this linker flexibility, we anticipated seeing GFP masses at heterogenous distances from its binding site(s). However, instead we observed GFP always ~10 nm from the putative Gmf1-binding site on Arp2/3 (Fig. S2A), and the reason for this consistent distance remains unclear. To map a potential Gmf1 binding site(s) from which these GFP molecules stem, we combined all 2D projections, superimposed the aligned Arp2/3 complexes onto each other, mapped the GFP locations, and drew circles with a 10 nm radius (Fig. S2B); this accounts for the size of GMF, the maximal length of the linker, and the size of the GFP. Our analysis was consistent with the existence of two binding sites, one on the Arp2 subunit and one on the Arp3 subunit (Fig. S2B, open circles in cartoon). The mapping also agrees well with the crystal structure of GMF-bound Arp2/3 complex [14], in which GMF directly contacts the

ARPC1/p40 subunit, and with chemical crosslinking analysis, which identified a potential second GMF-binding site on Arp3 [13].

GMF and Coronin synergize in inhibiting actin nucleation by Arp2/3 complex

Given that Coronin and GMF are conserved from yeast to mammals and appear to have separate binding sites on Arp2/3 complex, we asked whether these two proteins can work together to inhibit Arp2/3 complex-mediated actin nucleation. To test this, we used the VCA domain of yeast WASP (Las17) to activate yeast Arp2/3 complex in bulk fluorescence assays in the presence and absence of different concentrations of Gmf1 and/or Crn1. 250 nM Crn1 and 100 nM Gmf1 each modestly inhibited Arp2/3-dependent actin nucleation, but together abolished VCA-Arp2/3 complex activity (Fig. 3A). Further, at a fixed concentration of Crn1 that has modest inhibitory effects (250 nM), Gmf1 further inhibited nucleation in a concentration-dependent manner (Fig. 3B). Combined inhibitory effects were also observed when full-length Las17 was used instead of VCA domain to activate Arp2/3 complex (Fig. 3C); however, this required higher concentrations of the inhibitors, consistent with Las17 being a much stronger NPF than VCA [38, 39]. We also observed that the inhibitory effects of Gmf1 and Crn1 on Arp2/3 complex appear to be synergistic rather than additive. This raises the possibility that binding of one inhibitor could positively affect interactions of the other. Consistent with this view, 2D-classification analysis showed that the fraction of Arp2/3 particles with visible Crn1 bound increases by 3-fold in the presence of Gmf1 (Fig. 3D).

The structure of Arpin-bound Arp2/3 complex

Next, we asked where Arpin binds on the surface of Arp2/3 complex in relationship to GMF and Coronin, since each inhibitor induces an open conformation (Fig. 1B). The structure of Arpin (25 kDa) was recently solved by small-angle X-ray scattering (SAXS) and shown to be comprised of an N-terminal non-spherical globular domain connected by a linear tail (20 residues) to a short acidic (A) motif at its C-terminus [16, 40]. We generated 2D projection classes for Arpin-bound Arp2/3 complexes (Fig. 4A, upper panel), and compared them to ligand-free complex (Fig. 1A). This revealed that Arpin-bound complexes have either one or two new masses in each representative class average (yellow and white arrows, respectively, Fig. 4A, upper panel). In most of the class averages, there was a single new mass (yellow arrows, Fig. 4A, upper panel), while in some there were two new masses (white arrows, Fig. 4A, upper panel).

As a fully extended polypeptide chain, the linear tail of Arpin would span 3–6 nm, and indeed, we detected additional masses (~1.5 nm in diameter) located about 3 nm from the surface of Arp2/3 complex. Using the same strategy by which we mapped Gmf1-GFP binding sites on Arp2/3 complex, we identified two potential Arpin-binding sites, one located near the interface of the Arp3 and ARPC2/p35 subunits, and the other near the interface of Arp2 and Arp3 subunits (cartoon in Fig. 4A, open circles). Unlike Gmf1-GFP, Arpin was untagged; however, its globular core provided sufficient mass to serve as the tag.

To help clarify the positions of Arpin on Arp2/3 complex, we solved the 3D structure of Arpin-bound Arp2/3 complex (Fig. 4B) and compared it to ligand-free Arp2/3 complex (Fig.

4C). This revealed two main difference peaks, both located near the Arp2 subunit (pink shading in Fig. 4B; also see difference maps in Fig. S3B). These two new masses likely correspond to globular domains of two Arpin molecules. Taking into account the linear tails connecting these masses to the Arp2/3-interacting A motifs, the positions of these masses are consistent with predicted binding of the A motifs of Arpin to Arp2 and Arp3. Binding of Arpin may be stronger to Arp2 than Arp3, because all of our 2D projections showed an additional mass at this location, whereas some lacked an additional mass at the second location. We also note that Arpin binding appears to induce changes in the position of the p35/ARPC2 subunit, shifting it counter-clockwise (Fig. S3B).

DISCUSSION

The Arp2/3 complex is a conserved nucleator of branched actin filament networks. A number of studies have addressed the structural changes in Arp2/3 complex that accompany its co-activation by NPFs [20, 28, 41] and mother filaments [19]. Although Arp2/3 complex alone (no NPF) has some nucleation activity, strong nucleation requires binding of two VCA molecules to distinct surfaces on Arp2/3 complex [28–30]. At the suggested high-affinity site, the ‘A’ motif of VCA binds to the interface between Arp2 and ARPC1/p40 subunits [28], while the C motif binds Arp2 [30]. At the suggested low-affinity site, both the A and C motifs bind to the back of Arp3 [30]. The V motifs (or WH2 domains) of each VCA molecule recruit actin monomers, a critical step in nucleation, which become the first two conventional subunits of the daughter filament. Thus, nucleation appears involves formation of a pseudo-symmetrical complex with two VCAs binding opposite sides of Arp2/3 [28]. In contrast to this detailed understanding of Arp2/3 activation, there have been few structural studies to date addressing Arp2/3 inhibition [13, 21], and only one that has provided the 3D structure of the complex bound to an inhibitory protein [14].

In this study, we used single particle electron microscopy to obtain 2D and/or 3D models of Arp2/3 complex bound to its three established inhibitors: GMF, GST-Crn1, and Arpin. Our results suggest that the inhibitors bind to distinct surfaces on Arp2/3 complex, and that GMF and Arpin each have two binding sites on the complex, analogous to VCA. Coronin appears to bind to the ARPC2/p35 subunit. Arpin apparently binds to the two VCA-interacting surfaces on Arp2/3 complex, consistent with its inhibitory effects being dependent on it's A motifs. GMF binds to the interface between Arp2 and ARPC1/p40 subunits, and possibly to a second site on Arp3. Despite these differences in where they bind, each inhibitor induces one or more ‘open’ conformations in the Arp2/3 complex. Importantly, this suggests that diverse regulatory inputs can produce structurally and functionally related effects on Arp2/3 complex. Further, it raises the possibility of multiple inhibitors interacting simultaneously with the Arp2/3 complex, and indeed, GMF and Coronin acted synergistically to inhibit Arp2/3 complex in vitro (Fig. 3), and Arpin combinatorially inhibited Arp2/3 complex with GMF or Coronin (Fig. 4D). Thus, having multiple inhibitors with non-overlapping binding sites on Arp2/3 complex may provide cells with increased versatility by which to spatially and temporally tune actin nucleation activity. Another important implication of these results is that they suggest Arp2/3 complex may serve as a coincidence detector, receiving and integrating inhibitory signals from multiple pathways. This idea is particularly intriguing

because the WASP/WAVE family of Arp2/3-activating proteins are also coincidence detectors, but instead receive and integrate multiple stimulatory signals [42].

GMF induces a novel open conformation in Arp2/3 complex

We solved two distinct 3D structures of GMF-bound Arp2/3 complex (Fig. 2C & 2D). One structure adopts the 'standard open' conformation and has a new mass (the approximate size of GMF) at a location consistent with the GMF-Arp2/3 co-crystal structure [12]. The second structure has a novel open conformation and lacks a new mass at the first GMF binding site, but has additional mass at a second site. This second site is on Arp3, which agrees with previous anisotropy, binding saturation analysis, and chemical cross-linking experiments [13]. Given that the majority of GMF-bound particles (~85%) fell into the first category, i.e., the standard open conformation, and fewer fell into the second category, i.e., the novel open conformation, GMF may have higher affinity for the first binding site [14]. These results have important implications for the GMF mechanism. The new open conformation induced by GMF is highly incompatible with mother filament binding, and even the standard open conformation induced by GMF may interfere with filament side binding. Structural analysis of branch junctions suggests that most if not all subunits in the Arp2/3 complex interact with the mother filament to some degree [19], with subunits ARPC1, ARPC2 and ARPC4 making the most extensive interactions. In the novel open conformation induced by GMF, there are massive structural rearrangements, including a major shift of ARPC3 away from Arp2 and toward Arp3, which may render the complex less capable of binding the mother filament. Some of these structural changes may underlie GMF's ability to catalyze daughter filament dissociation from mother filaments [12, 13]. However, the structures we have solved here are for ligand-bound Arp2/3 complex in solution (without actin), and Arp2/3 complex found in actin filament branch junctions has a distinct conformation. Further, while GMF induces debranching, Crn1 and Arpin do not, yet all three induce open conformations. Therefore, it is not yet clear how our findings relate to GMF's debranching function.

Arpin binds two sites on Arp2/3 complex and induces the standard open conformation

Arpin (25 kDa) contains an Acidic (A) motif, which is required for its ability to inhibit Arp2/3 complex [40], and thus has been proposed to inhibit Arp2/3 complex by blocking VCA interactions. Our structural data are consistent with Arpin competing with VCA, but further reveal that Arpin binding influences the conformation of Arp2/3 complex, thus inhibiting nucleation in a manner not anticipated by a purely competitive binding model. Our 3D structure of Arpin-bound Arp2/3 complex shows that Arpin induces a standard open/inactive conformation, and supports the view that there are two Arpin binding sites on Arp2/3 complex (Fig. 4A & 4B; Fig. S3B), possibly corresponding to the two VCA binding sites. One Arpin density (presumably its globular core) contacts Arp2, while the other Arpin density sits closer to the backside of Arp3 where VCA interacts [27, 28]. These observations are also consistent with Arpin's inhibitory effects being less potent (micromolar range IC_{50}) compared to GMF and Coronin, even on mammalian Arp2/3 complex [40]. Effective inhibition may require binding of two Arpin molecules to block both VCA interactions. This scheme may enable cells to use Arpin to fine-tune VCA effects on Arp2/3 complex at the leading edge and/or allow Arpin to function in concert with other inhibitors to more fully block Arp2/3 activity.

Conclusions

Previous studies have shown that activation of the Arp2/3 complex is accompanied by structural rearrangements that close the gap between its Arp2 and Arp3 subunits, bringing them into closer register to stimulate daughter filament nucleation [4, 5]. These conformational changes induced by NPF binding are thought to 'prime' the Arp2/3 complex for nucleation, but additional steps are needed, including a second set of conformational changes that are suggested to occur when the primed complex interacts with the side of the mother filament [19, 43]. By comparison, there has been limited understanding of how inhibitors affect the structure of Arp2/3 complex. We previously showed that yeast and bovine Arp2/3 complexes (without ligands) each exist in an equilibrium between open and closed conformations [21], and that NPF binding stabilizes the closed state, whereas the inhibitor Coronin stabilizes the open state. In this study, we have shown that second inhibitor, Arpin, induces a related open/inhibitory conformation, and that a third inhibitor, GMF, induces both the standard open conformation and a strikingly different new open conformation. Together, these observations suggest that different inhibitors with different binding sites can induce similar open conformations, and that the Arp2/3 complex is capable of adopting a wide range of conformational/functional states. Indeed, this concept is supported by molecular dynamics simulations studies [44, 45]. Integration of this new information on inhibitors with existing knowledge of activators should provide a more complete view of how the activities of the Arp2/3 complex are locally controlled and fine-tuned by the concerted effects of multiple cellular ligands.

MATERIALS AND METHODS

Protein purification

Yeast Arp2/3 complex, full-length Las17 (WASP) and GST-VCA from Las17 were each purified as described [21]. Wild-type yeast GMF (Gmf1) and Gmf1-GFP were expressed as GST-fusion proteins in *E. coli* and purified by glutathione affinity chromatography, then treated with PreScission Protease (GE Healthcare) to remove the GST tag. Gmf1 proteins were further purified on a SOURCE 15Q column and then on a Superdex 200 column equilibrated in HEK buffer (20 mM Hepes pH 7.5, 1 mM EGTA, 50 mM KCl). GST-Crn1 was purified as described [46], and the GST tag was intentionally not removed. Multi-tagged human GST-6His-Arpin was expressed in *E.coli*, purified using Nickel affinity chromatography, and digested with TEV protease to remove both tags. Arpin was further purified and concentrated on a Resource Q column (GE healthcare), and dialyzed against buffer (20 mM Tris pH 7.5, 30 mM NaCl, 1 mM DTT). All proteins were flash frozen in aliquots in liquid nitrogen and stored at −80°C until use.

Actin Assembly Kinetics

Gel-filtered monomeric skeletal muscle actin in G-buffer (10 mM Tris pH 7.5, 0.2 mM $CaCl_2$, 0.2 mM DTT, 0.2 mM ATP) was cleared by ultracentrifugation at 90,000 rpm for 1 h at 4°C in a TLA100 rotor (Beckman Coulter; Indianapolus, IN). Each reaction (60 μl) contained 2 μM G-actin (5% pyrene labeled). To initiate polymerization, G-actin was converted to Mg^{2+}-ATP-actin, and then 2 min later, 42 μl G-actin was added to 15 μl of the indicated proteins/buffer, and mixed with 3 μl initiation mix (40 mM $MgCl_2$, 10 mM ATP, 1

M KCl). Fluorescence was monitored in a spectrophotometer (Photon Technologies International) at excitation and emission wavelengths of 365 and 407 nm, respectively.

Electron microscopy and image analysis

Arp2/3 complexes bound to Gmf1, GST-Crn1, or Arpin (gels of purified proteins in Fig. S6) were prepared by incubating for 30–60 min a ten-fold excess of ligand with immobilized HA-tagged Arp2/3 complex still attached to anti-HA antibody-coated beads, then washing the beads and releasing the complexes by TEV protease digestion for 30 min at room temperature [47]. The concentrations of Arp2/3 complex and regulators used were optimized in previous studies for their effects in functional assays and for single particle EM [13, 21, 47]. Freshly eluted complexes were applied to carbon-coated glow-discharged copper EM grids, then negatively stained with 0.75% Uranyl formate for 30 sec, air-dried, and analyzed in a JEOL 2100 electron microscope at 200 kV at low-dose conditions (Fig. S4). For random conical tilt method, the grids were tilted at 45 degree angles, and images captured with a Ultrascan 1000XP CCD (Gatan) at 40,000× magnification and 1.5–2.8 μm underfocus. To obtain a tilt pair of images, the same field of view was imaged without tilting. In this manner, pairs of corresponded images were obtained for each sample: 1500 pairs for Arp2/3 complex alone, 2400 Arp2/3 complex with Gmf1, and 2500 for Arp2/3 complex with Arpin. The corresponded tilted and untilted views of each complex were collected manually in BOXER [48]. A total of 1250 untilted views of GST-Crn1-bound Arp2/3 particles were collected using BOXER. Correction for the contrast transfer function (CTF) of the microscope was done in EMAN2.1 [48].

Untilted particles were processed using the IMAGIC5 package [49] as described in [21]. Briefly, all particles were filtered, normalized and subject to reference-free classification, followed by several rounds of multi-reference alignment. The final dataset had 50 classes, which were assigned to different conformations (open or closed), based on the existence of the cleft between Arp2 and Arp3 subunits. Particles attributed to each conformation, were extracted from the dataset, using IMAGIC5 command *msa-extract* and corresponded numbers were plotted on the graph. Difference maps between Arp2/3 complex structures with and without bound inhibitors were calculated after scaling each projection structure to give the same variance and zero mean. The Fourier ring correlation, calculated between projection structures that each included one half of the data, was used to estimate the resolution of the projection structures. The resolution of all structures was estimated at 25 Å, corresponding to approximately the first zero of the CTF of the electron microscope.

The preliminary 3D reconstructions of Arp2/3 complex bound to Gmf1 and bound to Arpin were generated in EMAN2.1 [48], using the Random Conical Tilt method and C1 symmetry. Subsequent refinement of the 3D structures was done in Frealign [50]. Statistical analysis revealed that single particles possess different orientations (Fig. S5D, S5D & S5F). For solving the 3D structure of Arpin-bound Arp2/3 complex (Fig. 4B), over 1000 additional untilted particles were added to the data set before refinement in Frealign. The resulting 3D structures of the ligand-bound Arp2/3 complexes had a resolution of 23–28 Å, estimated by the Fourier Shell Correlation method (Fig. S5G & S5H). 3D difference mapping was performed with UCSF Chimera [51], in which we used the crystal structure of GMF-bound

Arp2/3 complex (pdb code 4JD2), and calculated its 3D structure at 20 Å resolution using command *molmap*, then calculated difference maps between Arp2/3 complexes with and without different inhibitors using command *vop subtract*.

Supplementary Material

Refer to Web version on PubMed Central for supplementary material.

Acknowledgments

Electron microscopy was performed at the User facilities center of Biology department of M.V. Lomonosov Moscow University. O.S.S. and members of her lab were supported by a grant from the Russian Science Foundation (14-14-00234). S.B.P. was supported by grants to Michael K. Rosen from the HHMI, the NIH (R01-GM56322) and the Welch Foundation (I–1544). B.L.G and members of his lab were supported by a grant from the NIH (GM063691) to B.L.G.

Abbreviations

EM	electron microscopy
NPF	nucleation-promoting factor
FSC	Fourier Shell Correlation
CTF	contrast transfer function
RCT	random conical tilt
GMF	glia maturation factor

LITERATURE

1. Pollard TD, Borisy GG. Cellular motility driven by assembly and disassembly of actin filaments. Cell. 2003; 112:453–465. [PubMed: 12600310]
2. Kaksonen M, Toret CP, Drubin DG. Harnessing actin dynamics for clathrin-mediated endocytosis. Nat Rev Mol Cell Biol. 2006; 7:404–414. [PubMed: 16723976]
3. Rotty JD, Wu C, Bear JE. New insights into the regulation and cellular functions of the ARP2/3 complex. Nat Rev Mol Cell Biol. 2013; 14:7–12. [PubMed: 23212475]
4. Pollard TD. Regulation of actin filament assembly by Arp2/3 complex and formins. Annu Rev Biophys Biomol Struct. 2007; 36:451–477. [PubMed: 17477841]
5. Goley ED, Welch MD. The ARP2/3 complex: an actin nucleator comes of age. Nat Rev Mol Cell Biol. 2006; 7:713–726. [PubMed: 16990851]
6. Firat-Karalar EN, Welch MD. New mechanisms and functions of actin nucleation. Curr Opin Cell Biol. 2011; 23:4–13. [PubMed: 21093244]
7. Higgs HN, Pollard TD. Regulation of actin filament network formation through ARP2/3 complex: activation by a diverse array of proteins. Annu Rev Biochem. 2001; 70:649–676. [PubMed: 11395419]
8. Humphries CL, Balcer HI, D'Agostino JL, Winsor B, Drubin DG, Barnes G, et al. Direct regulation of Arp2/3 complex activity and function by the actin binding protein coronin. J Cell Biol. 2002; 159:993–1004. [PubMed: 12499356]
9. Cai L, Makhov AM, Schafer DA, Bear JE. Coronin 1B antagonizes cortactin and remodels Arp2/3-containing actin branches in lamellipodia. Cell. 2008; 134:828–842. [PubMed: 18775315]
10. Foger N, Rangell L, Danilenko DM, Chan AC. Requirement for coronin 1 in T lymphocyte trafficking and cellular homeostasis. Science. 2006; 313:839–842. [PubMed: 16902139]

11. Liu SL, Needham KM, May JR, Nolen BJ. Mechanism of a concentration-dependent switch between activation and inhibition of Arp2/3 complex by coronin. J Biol Chem. 2011; 286:17039–17046. [PubMed: 21454476]
12. Gandhi M, Smith BA, Bovellan M, Paavilainen V, Daugherty-Clarke K, Gelles J, et al. GMF is a cofilin homolog that binds Arp2/3 complex to stimulate filament debranching and inhibit actin nucleation. Curr Biol. 2010; 20:861–867. [PubMed: 20362448]
13. Ydenberg CA, Padrick SB, Sweeney MO, Gandhi M, Sokolova O, Goode BL. GMF severs actin-Arp2/3 complex branch junctions by a cofilin-like mechanism. Curr Biol. 2013; 23:1037–1045. [PubMed: 23727094]
14. Luan Q, Nolen BJ. Structural basis for regulation of Arp2/3 complex by GMF. Nat Struct Mol Biol. 2013; 20:1062–1068. [PubMed: 23893131]
15. Maritzen T, Zech T, Schmidt MR, Krause E, Machesky LM, Haucke V. Gadkin negatively regulates cell spreading and motility via sequestration of the actin-nucleating ARP2/3 complex. Proc Natl Acad Sci U S A. 2012; 109:10382–10387. [PubMed: 22689987]
16. Dang I, Gorelik R, Sousa-Blin C, Derivery E, Guerin C, Linkner J, et al. Inhibitory signalling to the Arp2/3 complex steers cell migration. Nature. 2013; 503:281–284. [PubMed: 24132237]
17. Volkmann N, Amann KJ, Stoilova-McPhie S, Egile C, Winter DC, Hazelwood L, et al. Structure of Arp2/3 complex in its activated state and in actin filament branch junctions. Science. 2001; 293:2456–2459. [PubMed: 11533442]
18. Egile C, Rouiller I, Xu XP, Volkmann N, Li R, Hanein D. Mechanism of filament nucleation and branch stability revealed by the structure of the Arp2/3 complex at actin branch junctions. PLoS Biol. 2005; 3:e383. [PubMed: 16262445]
19. Rouiller I, Xu XP, Amann KJ, Egile C, Nickell S, Nicastro D, et al. The structural basis of actin filament branching by the Arp2/3 complex. J Cell Biol. 2008; 180:887–895. [PubMed: 18316411]
20. Xu XP, Rouiller I, Slaughter BD, Egile C, Kim E, Unruh JR, et al. Three-dimensional reconstructions of Arp2/3 complex with bound nucleation promoting factors. Embo J. 2012; 31:236–247. [PubMed: 21934650]
21. Rodal AA, Sokolova O, Robins DB, Daugherty KM, Hippenmeyer S, Riezman H, et al. Conformational changes in the Arp2/3 complex leading to actin nucleation. Nat Struct Mol Biol. 2005; 12:26–31. [PubMed: 15592479]
22. Martin AC, Xu XP, Rouiller I, Kaksonen M, Sun Y, Belmont L, et al. Effects of Arp2 and Arp3 nucleotide-binding pocket mutations on Arp2/3 complex function. J Cell Biol. 2005; 168:315–328. [PubMed: 15657399]
23. Mullins RD, Heuser JA, Pollard TD. The interaction of Arp2/3 complex with actin: nucleation, high affinity pointed end capping, and formation of branching networks of filaments. Proc Natl Acad Sci U S A. 1998; 95:6181–6186. [PubMed: 9600938]
24. Blanchoin L, Amann KJ, Higgs HN, Marchand JB, Kaiser DA, Pollard TD. Direct observation of dendritic actin filament networks nucleated by Arp2/3 complex and WASP/Scar proteins. Nature. 2000; 404:1007–1011. [PubMed: 10801131]
25. Amann KJ, Pollard TD. The Arp2/3 complex nucleates actin filament branches from the sides of pre-existing filaments. Nat Cell Biol. 2001; 3:306–310. [PubMed: 11231582]
26. Smith BA, Padrick SB, Doolittle LK, Daugherty-Clarke K, Correa IR Jr, Xu MQ, et al. Three-color single molecule imaging shows WASP detachment from Arp2/3 complex triggers actin filament branch formation. Elife. 2013; 2:e01008. [PubMed: 24015360]
27. Smith BA, Gelles J, Goode BL. Single-molecule studies of actin assembly and disassembly factors. Methods Enzymol. 2014; 540:95–117. [PubMed: 24630103]
28. Boczkowska M, Rebowski G, Kast DJ, Dominguez R. Structural analysis of the transitional state of Arp2/3 complex activation by two actin-bound WCAs. Nature communications. 2014; 5:3308.
29. Padrick SB, Doolittle LK, Brautigam CA, King DS, Rosen MK. Arp2/3 complex is bound and activated by two WASP proteins. Proceedings of the National Academy of Sciences of the United States of America. 2011; 108:E472–E479. [PubMed: 21676863]
30. Ti SC, Jurgenson CT, Nolen BJ, Pollard TD. Structural and biochemical characterization of two binding sites for nucleation-promoting factor WASp-VCA on Arp2/3 complex. Proceedings of the

National Academy of Sciences of the United States of America. 2011; 108:E463–E471. [PubMed: 21676862]

31. Goroncy AK, Koshiba S, Tochio N, Tomizawa T, Sato M, Inoue M, et al. NMR solution structures of actin depolymerizing factor homology domains. Protein Sci. 2009; 18:2384–2392. [PubMed: 19768801]
32. Poukkula M, Hakala M, Pentinmikko N, Sweeney MO, Jansen S, Mattila J, et al. GMF promotes leading-edge dynamics and collective cell migration in vivo. Curr Biol. 2014; 24:2533–2540. [PubMed: 25308079]
33. Haynes EM, Asokan SB, King SJ, Johnson HE, Haugh JM, Bear JE. GMFbeta controls branched actin content and lamellipodial retraction in fibroblasts. J Cell Biol. 2015; 209:803–812. [PubMed: 26101216]
34. Goode BL, Wong JJ, Butty AC, Peter M, McCormack AL, Yates JR, et al. Coronin promotes the rapid assembly and cross-linking of actin filaments and may link the actin and microtubule cytoskeletons in yeast. The Journal of cell biology. 1999; 144:83–98. [PubMed: 9885246]
35. Spoerl Z, Stumpf M, Noegel AA, Hasse A. Oligomerization, F-actin interaction, and membrane association of the ubiquitous mammalian coronin 3 are mediated by its carboxyl terminus. J Biol Chem. 2002; 277:48858–48867. [PubMed: 12377779]
36. Gatfield J, Albrecht I, Zanolari B, Steinmetz MO, Pieters J. Association of the leukocyte plasma membrane with the actin cytoskeleton through coiled coil-mediated trimeric coronin 1 molecules. Mol Biol Cell. 2005; 16:2786–2798. [PubMed: 15800061]
37. Goley ED, Rammohan A, Znameroski EA, Firat-Karalar EN, Sept D, Welch MD. An actin-filament-binding interface on the Arp2/3 complex is critical for nucleation and branch stability. Proc Natl Acad Sci U S A. 2010; 107:8159–8164. [PubMed: 20404198]
38. Rodal AA, Manning AL, Goode BL, Drubin DG. Negative regulation of yeast WASp by two SH3 domain-containing proteins. Curr Biol. 2003; 13:1000–1008. [PubMed: 12814545]
39. Sun Y, Martin AC, Drubin DG. Endocytic internalization in budding yeast requires coordinated actin nucleation and myosin motor activity. Dev Cell. 2006; 11:33–46. [PubMed: 16824951]
40. Fetics S, Thureau A, Campanacci V, Aumont-Nicaise M, Dang I, Gautreau A, et al. Hybrid Structural Analysis of the Arp2/3 Regulator Arpin Identifies Its Acidic Tail as a Primary Binding Epitope. Structure. 2016; 24:252–260. [PubMed: 26774128]
41. Goley ED, Rodenbusch SE, Martin AC, Welch MD. Critical conformational changes in the Arp2/3 complex are induced by nucleotide and nucleation promoting factor. Molecular cell. 2004; 16:269–279. [PubMed: 15494313]
42. Padrick SB, Rosen MK. Physical mechanisms of signal integration by WASP family proteins. Annu Rev Biochem. 2010; 79:707–735. [PubMed: 20533885]
43. Cai L, Bear JE. Peering deeply inside the branch. J Cell Biol. 2008; 180:853–855. [PubMed: 18316414]
44. Dalhaimer P, Pollard TD. Molecular dynamics simulations of Arp2/3 complex activation. Biophys J. 2010; 99:2568–2576. [PubMed: 20959098]
45. Pfaendtner J, Voth GA. Molecular dynamics simulation and coarse-grained analysis of the Arp2/3 complex. Biophys J. 2008; 95:5324–5333. [PubMed: 18805923]
46. Gandhi M, Achard V, Blanchoin L, Goode BL. Coronin switches roles in actin disassembly depending on the nucleotide state of actin. Mol Cell. 2009; 34:364–374. [PubMed: 19450534]
47. Ydenberg CA, Smith BA, Breitsprecher D, Gelles J, Goode BL. Cease-fire at the leading edge: new perspectives on actin filament branching, debranching, and cross-linking. Cytoskeleton. 2011; 68:596–602. [PubMed: 22002930]
48. Ludtke SJ, Baldwin PR, Chiu W. EMAN: Semiautomated software for high-resolution single-particle reconstructions. J Struct Biol. 1999; 128:82–97. [PubMed: 10600563]
49. van Heel M, Harauz G, Orlova EV, Schmidt R, Schatz M. A new generation of the IMAGIC image processing system. J Struct Biol. 1996; 116:17–24. [PubMed: 8742718]
50. Grigorieff N. FREALIGN: high-resolution refinement of single particle structures. J Struct Biol. 2007; 157:117–125. [PubMed: 16828314]
51. Goddard TD, Huang CC, Ferrin TE. Visualizing density maps with UCSF Chimera. J Struct Biol. 2007; 157:281–287. [PubMed: 16963278]

Research highlights

- Coronin, GMF, and Arpin each induce related open conformations in Arp2/3 complex
- GMF binding induces two distinct inhibitory states of Arp2/3 complex
- Coronin, GMF, and Arpin combinatorially inhibit Arp2/3 complex activity
- Arpin has two separate binding sites on Arp2/3 complex Arp2 and Arp3

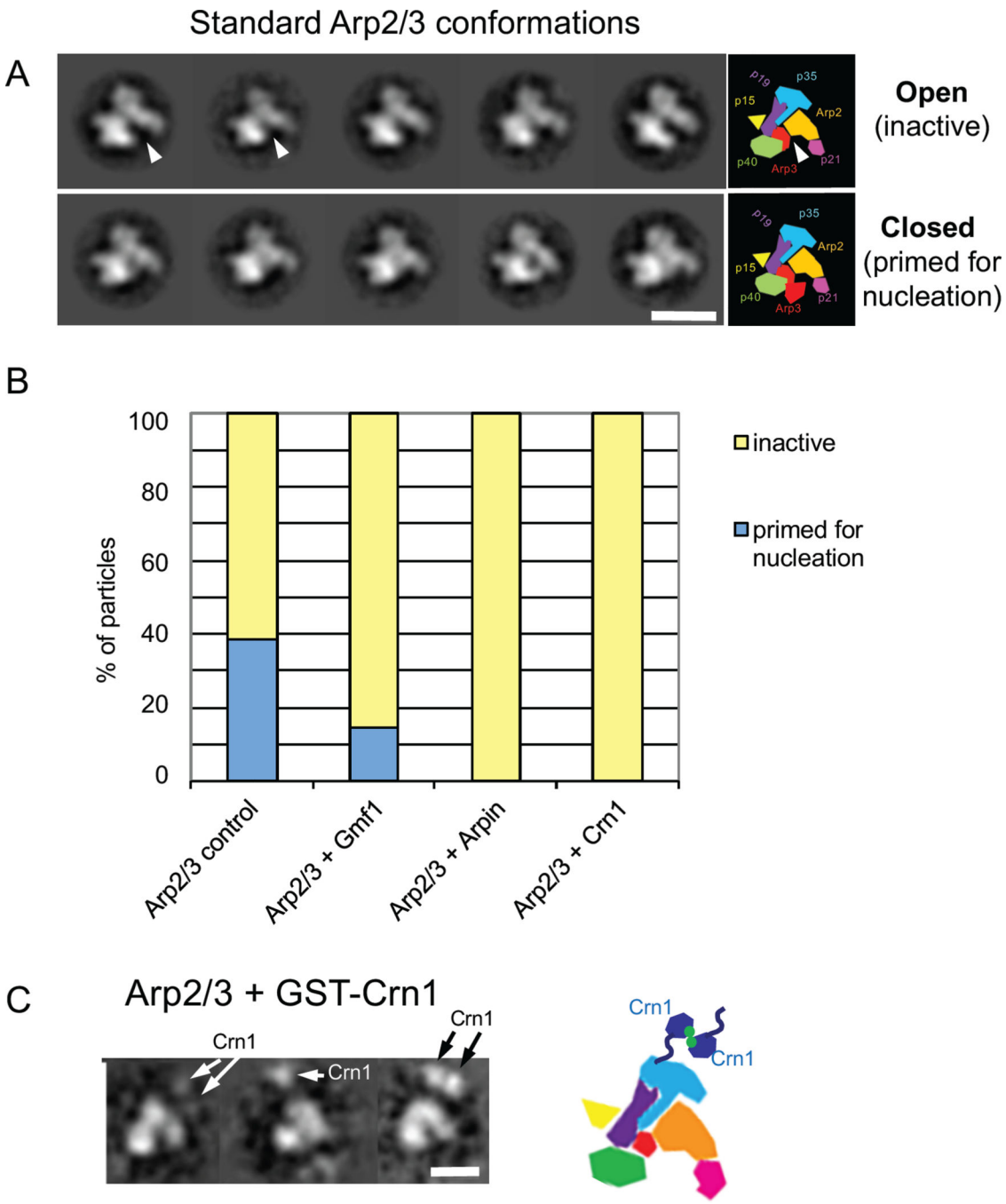

Figure 1. Distribution of Arp2/3 complex conformations in ligand-bound and unbound states

(A) Two-dimensional projections of 'standard' open and closed conformations of ligand-free Arp2/3 complex. Upper row, representative class averages of open conformation. Bottom row, representative class averages of closed conformation. Scale bar, 10 nm. Arrowheads point to the cleft between Arp2 and Arp3 in the open conformation. Cartoon panels in each row show the 7 subunits of Arp2/3 complex with color-coding as in all other figures: Arp2, red; Arp3, orange, ARPC1/p40, green, ARPC2/p35, blue; ARPC3/p21, light purple; ARPC4/p19, dark purple; ARPC5/p15, yellow. (B) Percentage of Arp2/3 complex particles

in the open (inactive) versus closed (primed for nucleation) conformations (Arp2/3, $n = 262$; Arp2/3+Gmf1, $n = 731$; Arp2/3+Arpin, $n = 1130$; Arp2/3+Crn1, $n = 362$). (C) Two-dimensional projections of GST-Crn1 bound to Arp2/3 complex (left). Arrows highlight the visible new masses, which likely represent the globular β-propeller domains of a Crn1 dimer. Scale bar, 10 nm. Cartoon (right) depicts proposed arrangement of two Crn1 molecules (dark blue) dimerized by GST (green dots), with one Crn1 molecule in the dimer interacting with the p35/ARPC2 subunit of Arp2/3 complex.

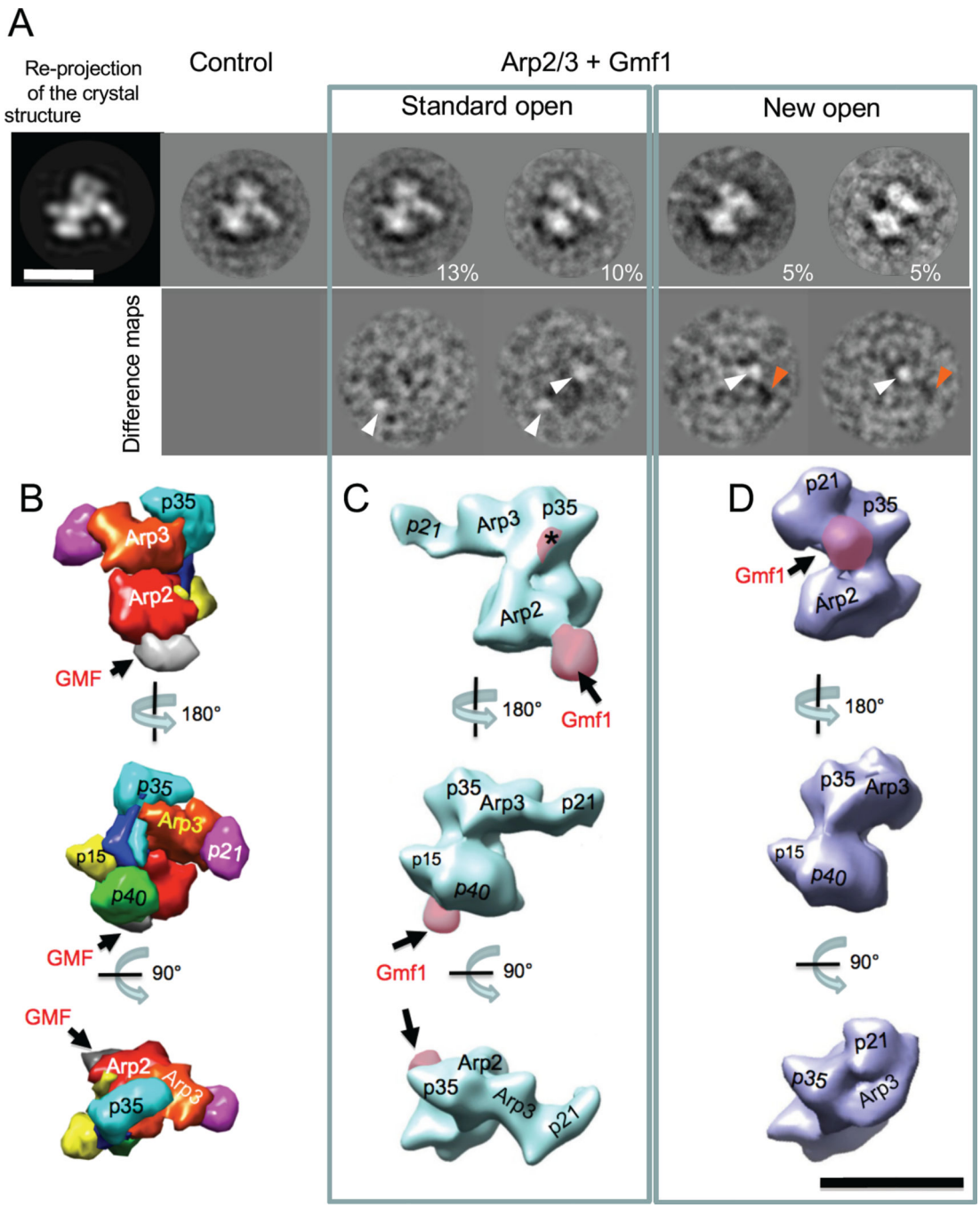

Figure 2. Three-dimensional structures of Gmf1-bound Arp2/3 complexes

(A) Two-dimensional projections of Gmf1-bound Arp2/3 complex. Upper row, from left to the right: re-projection of the crystal structure of Arp2/3-GMF complex [14], free Arp2/3 2D projection in the same orientation, two representative 2D projections of Arp2/3-Gmf1 in standard open conformation, and two 2D projections of Arp2/3-Gmf1 in new open conformation. Numbers on the right reflect % of the particles in each class. Bottom row: difference maps, generated by subtracting the 2D projection of free Arp2/3 from Arp2/3-Gmf1 projections, respectively. White arrowheads highlight adding of the new mass, orange

arrowheads highlight loss of the mass. (B) Crystal structure of GMF-bound Arp2/3 complex [14] filtered to 25 Å resolution using UCSF Chimera [51]. Arp2/3 complex subunits, color-coded and labeled as in Figure 1A. Arrows highlight the position of GMF (grey) bound to Arp2 and p40/ARPC1 subunits. (C,D) Three-dimensional reconstructions of Gmf1-bound Arp2/3 complex in the standard open conformation (C) and the new open conformation (D). Additional densities, approximately the size of Gmf1, are shaded in pink and labeled with arrows. Asterisk in (C) marks a new mass at the proposed second binding site for GMF on Arp3. Three separate views of Arp2/3 complex shown in B-D are aligned to each other for comparison. Scale bar, 10 nm.

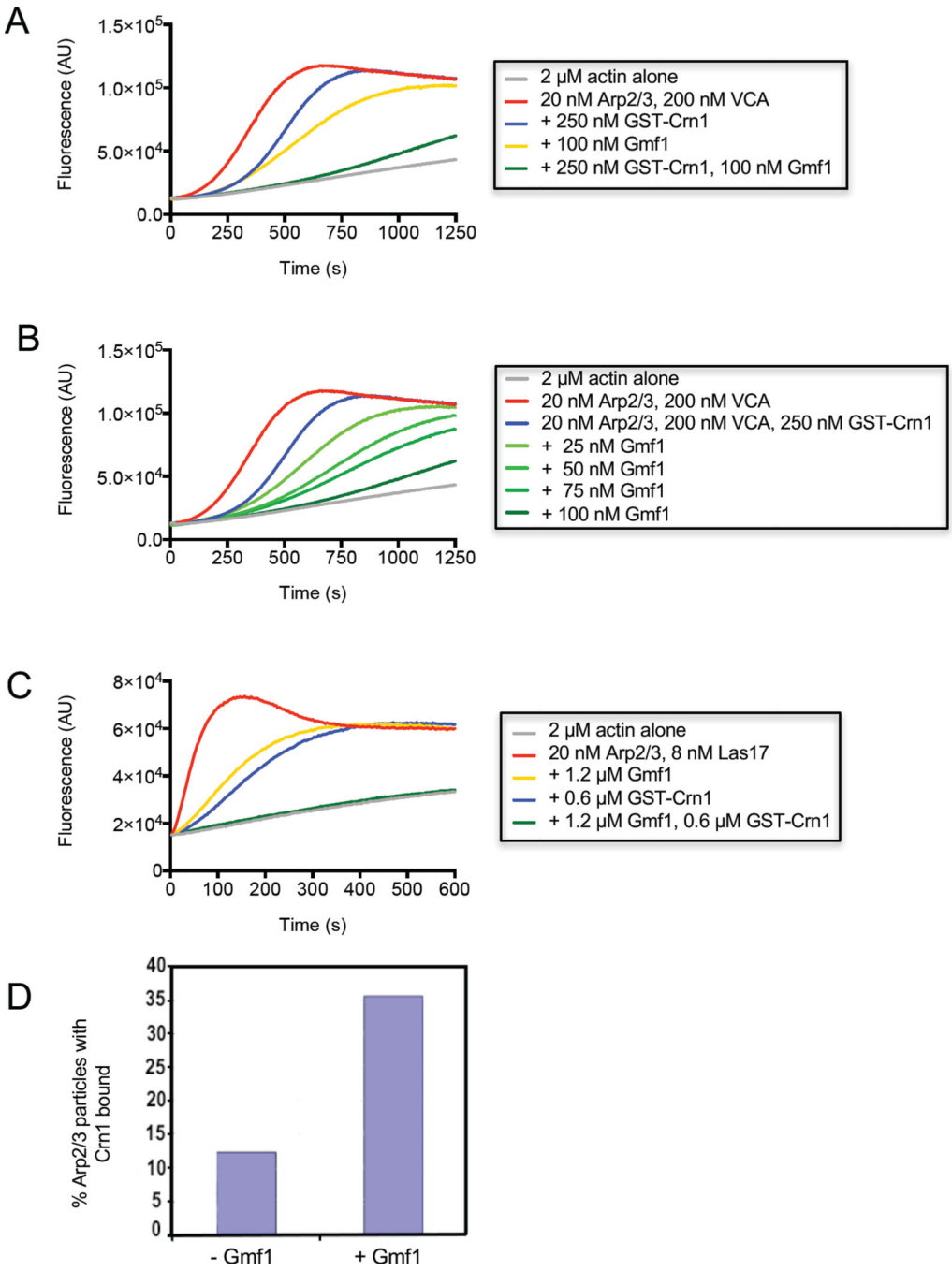

Figure 3. Gmf1 and Crn1 synergize in inhibiting Arp2/3-mediated actin assembly in vitro

(A, B) Bulk actin polymerization assays containing G-actin (2 μM, 5% pyrene-labeled) and the indicated concentrations of Arp2/3 complex, VCA, Gmf1, and Crn1. (C) Bulk actin polymerization assays, performed as in A and B, except using full-length Las17 (yeast WASP) instead of VCA. (D) Percentage of Arp2/3 complex particles with Crn1 bound in the presence and absence of Gmf1 (- Gmf1, $n = 366$; + Gmf1, $n = 398$).

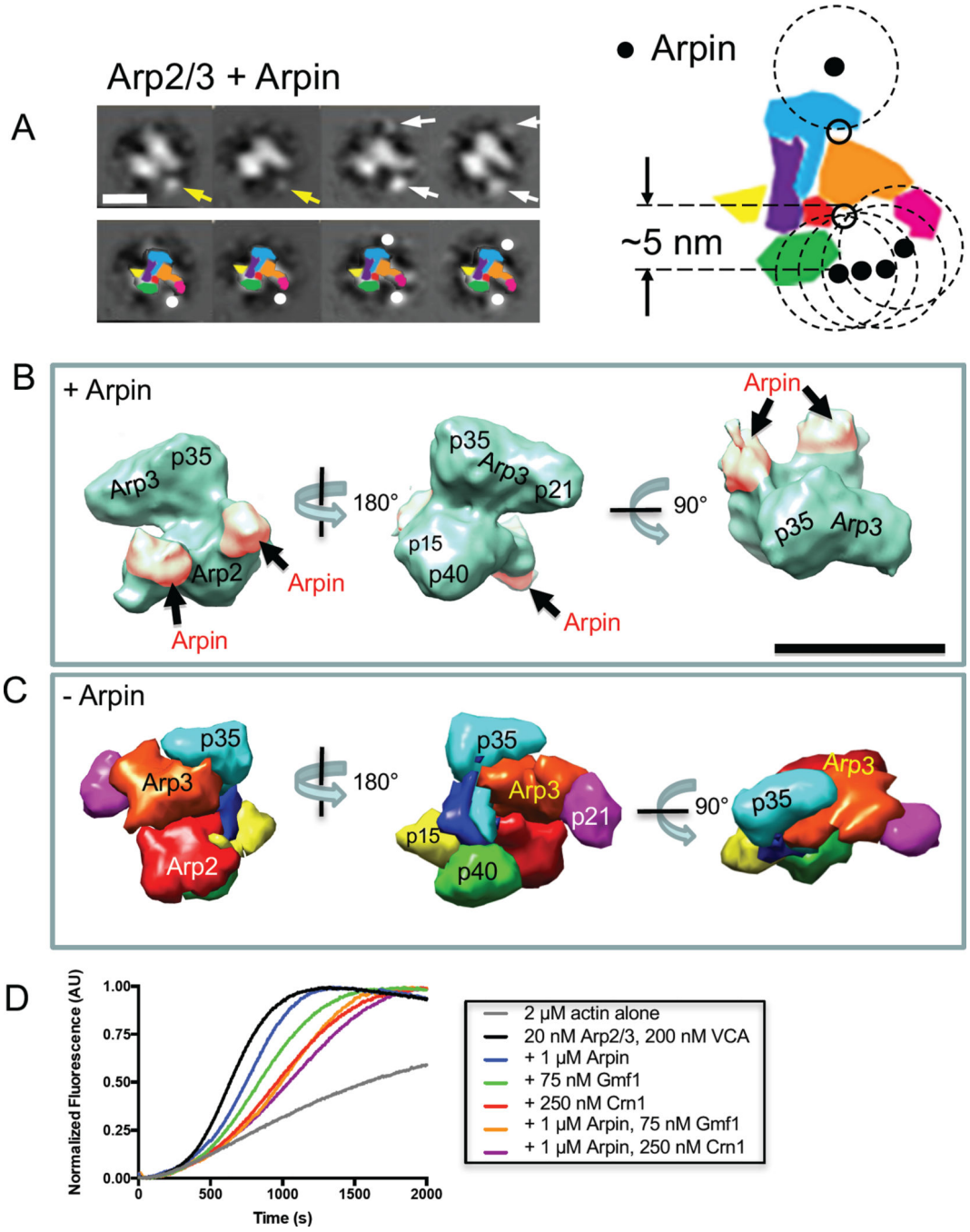

Figure 4. Three-dimensional structure of Arpin-bound Arp2/3 complex

(A) Two-dimensional projections of Arpin-bound Arp2/3 complex. Arrows highlight new masses, which likely represent the globular core domains of Arpin [40]. Yellow arrows indicate the presence of a single new mass, while white arrows indicate two new masses. Scale bar, 10 nm. Lower panel includes corresponding cartoons of each class average. The larger cartoon on the right shows Arp2/3 complex with superimposed positions of Arpin (filled circles). Dashed circles have a 5 nm radius, corresponding to the estimated length connecting the center of Arpin globular domain and its C-terminal acidic (A) motif. The

circles were used to map potential Arpin-binding sites on Arp2/3 complex (open circles). (B) Three-dimensional reconstruction of Arpin-bound Arp2/3 complex viewed from different angles. Additional density, attributed to Arpin, is shaded pink. (C) Crystal structure of Arp2/3 complex [14] filtered to 25 Å resolution using UCSF Chimera [51], with subunits color-coded and labeled. Views are aligned with those in B for comparison. Scale bar, 10 nm. (D) Bulk actin polymerization assays containing G-actin (2 μM, 5% pyrene-labeled) and the indicated concentrations of Arp2/3 complex, VCA, Arpin, Gmf1, and Crn1.